Published in final edited form as:
AIDS. 2012 July 31; 26(12): 1501–1508. doi:10.1097/QAD.0b013e3283550bec.

The Effects of HIV and Combination Antiretroviral Therapy on White Matter Integrity

Patrick Wright, BS[1,2], **Jodi Heaps, MS**[3], **Josh S. Shimony, MD, PhD**[4], **Jewell B. Thomas, BS**[2], and **Beau M. Ances, MD, PhD**[1,2]

[1]Department of Biomedical Engineering, Washington University in Saint Louis, Saint Louis, MO

[2]Department of Neurology, Washington University in Saint Louis, Saint Louis, MO

[3]Department of Psychology, University of Missouri Saint Louis, Saint Louis, MO

[4]Department of Radiology, Washington University in Saint Louis, Saint Louis, MO

Abstract

HIV preferentially affects white matter (WM) in the brain. While combination antiretroviral therapy (cART) reduces HIV viral load within the brain, continued inflammation can persist. Diffusion tensor imaging (DTI) provides a non-invasive method to assess WM structural integrity in the cART era. We examined the impact of HIV and cART on WM integrity within the corpus callosum (CC) and centrum semiovale (CSO) using DTI. Neuropsychological testing and DTI scans were acquired for a cross-sectional cohort consisting of 63 individuals that were divided into one of three groups: 21 HIV-uninfected (HIV-) controls, 21 HIV-infected (HIV+) subjects naïve to cART (HIV+/cART-), and 21 HIV+ subjects receiving stable cART (HIV+/cART+). DTI measures (fractional anisotropy (FA), mean diffusivity (MD), axial diffusivity (AD), radial diffusivity (RD)) were obtained for the genu, splenium, and body of the CC as well as the CSO. A subset of the HIV+/cART- individuals (n=10) were also longitudinally assessed immediately before and approximately 6 months after receiving stable therapy. Differences among the cross-sectional groups were assessed using an ANOVA while paired t-tests evaluated longitudinal changes. The HIV+/cART- participants had significantly lower MD, AD, and RD for each CC region and the CSO compared to HIV- controls and HIV+/cART+ individuals. Observed decreases in DTI parameters could reflect the presence of inflammatory cells or cytotoxic edema in the WM of HIV+/cART- subjects. No significant difference existed between HIV- controls and HIV+/cART+ subjects. In some HIV+ subjects, initiation of cART led to significant increases in MD, RD, and AD but not FA in the CC and CSO regions. Observed changes in DTI parameters in the WM after initiating cART could reflect reduced neuro-inflammation. Future DTI studies may be useful in evaluating the efficacy of cART regimens with higher brain penetration.

Keywords

HIV; Diffusion Tensor Imaging (DTI); Combination Antiretroviral Therapy (cART); Corpus Callosum (CC); Centrum Semiovale (CSO)

1. Introduction

Human immunodeficiency virus (HIV) quickly enters the brain soon after seroconversion and can subsequently result in cognitive impairment (Ances & Ellis, 2007). The introduction

Corresponding Author: Beau M. Ances, M.D. Ph.D., Box 8111, 660 South Euclid Avenue, St. Louis, MO 6311, bances@wustl.edu, Phone: 314-747-8423, Fax: 314-747-8427.

of combination antiretroviral therapy (cART) has greatly reduced the severity of central nervous system (CNS) damage, but cognitive impairment continues to occur despite the introduction of these medications (Narciso et al., 2001). HIV infected (HIV+) individuals receiving cART may continue to have persistent virus within the CNS resulting in neuro-inflammation and white matter (WM) abnormalities (Cardenas et al., 2009).

Diffusion tensor imaging (DTI) has become an increasingly popular method for studying *in vivo* WM structural integrity in neurodegenerative diseases (Bohanna et al., 2008; Ewers et al., 2011; Sullivan et al., 2011; Turner & Modo, 2010). DTI measures the diffusion of water molecules in WM. Movement of water can be anisotropic with diffusion greater along the length of the fiber (longitudinal direction) than perpendicular to it (radial or transverse direction), as myelin may restrict diffusion (Chanraud et al., 2010). Diffusion along the major axis is assumed to reflect diffusivity parallel to the white matter tract and is termed axial diffusivity (AD). The two minor axes can be averaged to determine radial diffusivity (RD), which reflects diffusion perpendicular to the white matter (Song et al., 2002). Mean diffusivity (MD) reflects the average diffusion from all three directions. Finally, fractional anisotropy (FA) is a value between zero and one and provides a measure of the general shape of the ellipsoid. A reduction in AD could represent axonal compromise, while decreases in RD may indicate myelin degradation (Kim et al., 2007; Naismith et al., 2010; Song et al., 2003).

While DTI has been used to study the effects of HIV on WM integrity, results have been variable (Filippi et al., 2001; Gongvatana et al., 2009, 2011; Kuper et al., 2011; Li et al., 2011; Muller-Oehring et al., 2010; Pfefferbaum et al., 2007, 2009; Pomara et al., 2001; Ragin et al., 2004a, 2004b, 2005; Stebbins et al., 2007; Tate et al., 2011; Thurnher et al., 2005; Towgood et al., 2011; Wu et al., 2006). In general many studies have shown increases in MD and decreases in FA within the corpus callosum (CC) and centrum semiovale (CSO) due to HIV. Filippi and colleagues showed a decrease in FA and an increase in MD in the genu and splenium of the CC of HIV+ patients (n=10; Filippi et al., 2001). Thurnher and colleagues also observed a reduction in FA due to HIV *but* within the genu of the CC (Thurnher et al., 2005). Furthermore, Wu and colleagues reported that HIV+ patients had a reduction in FA within the splenium of the CC compared to HIV- controls. A reduction in FA within the CC and CSO of HIV+ participants was associated with worsening motor speed performance (Wu et al., 2006). In a more recent study that focused on only on cortical regions within HIV+ individuals, an increase in MD and a decrease in FA were observed in the internal capsule, inferior longitudinal fasciculus, and optic radiation (Gongvatana et al., 2011).

Most studies have rarely assessed the impact of cART on WM integrity using DTI. Individuals have been typically classified according to serostatus, with HIV+ patients receiving cART (HIV+/cART+) and those naïve to cART (HIV+/cART-) merged into a single group. The few studies that have investigated the effects of cART on DTI parameters in HIV+ individuals have shown conflicting results. Pffeferbaum and colleagues demonstrated that HIV+/cART- individuals (n=9) had significantly higher RD values in the inferior cingulate bundle, occipital forceps and superior longitudinal fasciculus compared to HIV- controls (n=88) or HIV+/cART+ (n=33) (Pfefferbaum et al., 2009). However, Chen and colleagues noted no significant differences in DTI parameters between HIV+/cART- (n=11) and HIV+/cART+ (n=18) patients within subcortical brain regions (Chen et al., 2009). More recently, a decrease in FA was seen in the temporal lobes of HIV+/cART+ (n=69) compared to HIV+/cART- (n=16) individuals (Gongvatana et al., 2011). In general, relatively few HIV+/cART- individuals have been examined in these post-cART era studies.

In this study, we analyzed WM structural integrity within the genu, body, and splenium of the CC as well as the CSO of sixty-three participants (21 HIV- controls, 21 HIV+/cART-, and 21 HIV+/cART+). Within a subgroup of HIV-/cART- (n=10) we assessed the impact of therapy before and after commencing medications. We hypothesized that HIV+ participants naïve to cART may have significantly differences in DTI parameters compared to either HIV+ individuals receiving cART or HIV- controls. Also, we hypothesized that cART may modulate HIV-associated WM changes as seen in a longitudinal group that was followed both immediately prior to and approximately six months after starting therapy.

2. Materials and Methods

2.1 Subjects

Sixty-three participants were selected from ongoing studies. Each subject provided written consent approved by the Institutional Review Board at Washington University in Saint Louis. Individuals with a history of confounding neurological disorders including epilepsy, stroke, head injury with loss of consciousness greater than 30 minutes, major psychiatric disorders, or active substance abuse were excluded from participation. Serological status of all HIV+ participants was confirmed by documented positive HIV enzyme-linked immunoassay and Western blot or detection of plasma HIV RNA by polymerase chain reaction. All HIV+ participants had laboratory evaluations (plasma CD4 cell count and HIV RNA viral load) performed at the time of neuroimaging. The cohort was further divided into three groups and consisted of HIV- controls (n=21), HIV+/cART+ (n=21), or HIV+/cART- (n=21). In addition, a subgroup of the HIV+/cART- (n=10) was longitudinally assessed immediately before and approximately 6 months after receiving a stable regimen.

2.2 Medications

The specific regimens that HIV+/cART+ patients received included: nucleoside reverse transcriptase inhibitors (NRTIs) + non- nucleoside reverse transcriptase inhibitors (NNRTIs) (n=14), NRTIs+ protease inhibitors (PIs) (n=11), or NRTIs only (n=1). For the longitudinal study, HIV+ participants and their providers decided on the regimen. Within this longitudinal subgroup, HIV+ participants received the following regimens: NRTIs + NNRTIs (n=6) or NRTIs+ PIs (n=4). The ability of a particular antiretroviral (ARV) medication to penetrate across the blood brain barrier was classified using the central penetration effectiveness (CPE) score (Letendre et al., 2010). The score of each ARV in a participant's regimen was summed to calculate the total CPE value for a regimen.

2.3 Neuropsychological Evaluation

A brief neuropsychological performance battery that assessed memory, psychomotor speed, and executive function was administered to all participants. These measures have previously been used to assess HIV-associated neurocognitive disorder (Antinori et al., 2007; Tross et al., 1988; Van Gorp et al., 1989). Raw scores from each test were standardized using demographic (age, gender, race, education) adjusted normative means (Heaton et al., 1991, 2011; Robertson, 2009). A standardized z-score was calculated by subtracting the appropriate normative mean from the raw score and then dividing by the normative standard deviation. A composite neuropsychological summary *Z*-score (NPZ-4) was calculated by averaging *z*-scores from each test. For longitudinal assessments, alternate forms of the Hopkins Verbal Learning Test-Revised were administered. These different versions ensured that subjects were not influenced by previous exposure.

2.4 DTI Acquisition and Analysis

All scans were performed using a 3T Siemens Tim TRIO whole-body magnetic resonance scanner (Siemens AG, Erlangen, Germany) with a product transmit/receive head coil. A T1-

weighted three-dimensional magnetization-prepared rapid acquisition gradient echo (MPRAGE) sequence (Time of repetition (TR) /inversion time (TI)/ echo time (TE) = 2400/1000/3.16 ms, flip angle = 8°, and voxel size = 1 × 1 × 1 mm^3) was obtained. A T2-weighted fast spin echo (T2W FSE) scan (TR = 4380 ms, TE = 94 ms, 1 × 1× 3 mm) was also acquired. Images were visually inspected at the time of scanning and an additional scan was performed if significant motion artifacts were observed. Two acquisitions of diffusion-weighted images were collected for the assessment of white matter microstructural integrity (2 × 2 × 2 mm voxels, TR=9,900 ms, TE=102 ms, flip angle =90°, 23 directions with b-values between 0 and 1400 s/mm^2).

2.5 DTI Registration

A detailed review of the registration methods has been previously presented (Shimony et al., 2006). In brief, affine transforms computed by image registration were used to define the spatial relationships between all images. Multi-modal image registration between the anatomical images (T2W FSE and T1W MPRAGE) was accomplished using vector gradient measure (VGM) maximization (Rowland et al., 2005). The first DTI volume (I_0, with b = 0) was registered to the T2W FSE image, which was then registered to the T1W MPRAGE image, which in turn was subsequently registered to an atlas representative target that conformed to the Tailairach system (Lancaster et al., 1995; Tailairach et al., 1988).

2.6 DTI Motion Correction

The DTI dataset was motion corrected by first aligning each DTI volume to the geometric mean volume of each group of images that shared similar degrees of diffusion sensitization. The geometric mean volume was then recomputed before aligning to the first acquired I_0 image. Next, transforms between the different images were algebraically composed. Repeating these steps three times yielded realignments with errors that had an estimated internal consistency < 0.1 mm. All transforms were 9 parameter affine (rigid body + scanner axis stretch) computed by VGM maximization (Rowland et al., 2005). Conventional intensity correlation maximization was used to align the I_0 volumes of each DTI dataset. The final, motion corrected results were obtained by algebraically composing all transforms and averaging datasets after application of the composed transforms using cubic spline interpolation.

2.7 DTI Computations

DTI post-processing was performed using previously described methods (Shimony et al., 2009). Briefly, the diffusion tensor and its 3 eigenvalues were calculated using log-linear regression in each voxel (Basser et al., 1994). Using standard methods, the three eigenvalues were used to calculate RD, AD, and MD. Anisotropy was expressed as FA, which is normalized to assume a range from 0 to 1. Diffusion parameters were measured and sampled for each individual by averaging particular regions of interest within the CC and CSO.

2.8 Region of Interest Analysis

DTI parameters were obtained for the genu, body, and splenium of the CC and the CSO using manually drawn regions of interest (ROI) created in Analyze (Mayo Clinic, Rochester, MN) (Figure 1). ROIs for the CC were manually delineated by estimating anatomical boundaries agreed upon by two trained raters (PW and JH). The genu, body, and splenium of the CC were drawn on the mid-sagittal slice of each subject's fractional anisotropy map. Each region was sampled across five slices that were centered upon this slice. Each DTI parameter reflects the average of these five slices. ROIs for the bilateral CSO were also manually drawn in atlas space and were sampled from three axial slices superior to the lateral ventricles.

2.9 Statistical Analysis

Demographic variables (including gender and neuropsychological performance) were compared across groups using an analysis of variance (ANOVA). In addition, Student's t-tests were performed comparing clinical variables (CD4 cell count, CD4 nadir cell count, and $\log_{10}$ plasma HIV viral load (VL)) between HIV+/cART- and HIV+/cART+. DTI parameters were log-transformed to improve normality with the transformed values. These log-transformed values were subsequently used in all analyses. Pearson's correlation coefficients were computed to assess the relationship between DTI parameters in each of the ROIs and NPZ-4 scores. For each of the CC regions and the CSO, a one-way ANOVA was used to compare DTI parameters across groups for the cross sectional analysis. Significance was set at an uncorrected value of $p<0.05$. Paired Student t-tests were employed to compare the subset of 10 HIV+ individuals who had DTI and neuropsychological performance testing performed prior to and approximately 6 months after receiving stable cART.

3. Results

3.1 Participant Demographics

Cross sectional demographic variables for the three groups (HIV- controls, HIV+/cART-, HIV+/cART+) are shown in Table 1. There were no significant differences between the groups in regards to age, sex, or education. Neuropsychological performance (NPZ-4 score) was also similar for the three groups. The HIV+/cART+ group had significantly ($p<0.01$) lower $\log_{10}$ plasma VL and nadir CD4 cell count than the HIV+/cART- group. In general, HIV+/cART+ subjects had been infected longer than HIV+/cART- individuals. No significant differences in current CD4 cell count were seen between the two HIV+ groups.

3.2 HIV+/cART- had significant decreases in DTI parameters compared to HIV- controls and HIV+/cART+

As can be seen in Table 2, decreases in MD, AD, and RD ($p<0.01$) were seen for each of the CC regions as well as the CSO for the HIV+/cART- group compared to either HIV+/cART+ or HIV- control groups. No significant differences were seen between HIV+/cART+ and HIV- control subjects. Moreover, FA values were similar among all three groups. For the two HIV+ groups, DTI parameters did not correlate with either NPZ-4 measures or laboratory values (data not shown).

3.3 Initiation of cART in HIV+ individuals led to improvements in DTI parameters

For the ten HIV+ participants that were followed longitudinally, increases in MD, AD, and RD ($p<0.01$) were observed after starting medications. For some subjects observed MD, AD, and RD values in subjects that had recently received stable cART were comparable to those seen in HIV+ participants who had chronically received cART. Of note, significant changes that were seen primarily occurred within four of the ten subjects (Figure 2). No changes in FA were seen in the HIV+ participants after starting medications. In general, while MD, AD, and RD were inversely correlated with decreases in $\log_{10}$ plasma VL, none of these comparisons were significant. In addition, neuropsychological performance did not improve significantly, after starting medications ($p=0.425$).

4. Discussion

This study suggests that DTI parameters within the CC and CSO are reduced in HIV+ subjects naïve to cART. MD, AD, and RD can quickly improve in some HIV+ subjects after initiating stable cART. In particular, DTI parameters in some HIV+ individuals who recently received stable cART were comparable to those seen in HIV+ subjects on long-term

medication. Observed changes in DTI values did not correlate with typical laboratory or neuropsychological performance measures.

Loss of WM integrity due to HIV has been previously described (Filippi et al., 2001; Gongvatana et al., 2009, 2011; Kuper et al., 2011; Li et al., 2011; Muller-Oehring et al., 2010; Pfefferbaum et al., 2007, 2009; Pomara et al., 2001; Ragin et al., 2004a, 2004b, 2005; Stebbins et al., 2007; Tate et al., 2011; Thurnher et al., 2005; Towgood et al., 2011; Wu et al., 2006). Many studies using DTI have shown an increase in MD and a decrease in FA in HIV+ patients (Chang et al., 2008; Filippi et al., 2001; Pfefferbaum et al., 2007; Thurnher et al., 2005; Wu et al., 2006). Similar DTI changes have been seen in other neurodegenerative disorders including Alzheimer's disease (Bozzali et al., 2002) and multiple sclerosis (Naismith et al., 2009; Rimkus et al., 2011). In contrast, we observed a decrease in AD, MD, and RD and no changes in FA in HIV+ subjects who were naive to cART. Observed decreases in diffusivity measures (MD, AD, RD) are similar to other studies that have investigated cellular tumors (Stadnik et al., 2001), brain abscesses (Guzman et al., 2002), and metabolic disorders such as phenylketonuria (PKU) (White et al., 2010). Our understanding of the microscopic correlates of these DTI changes remains incomplete but may vary for these disorders. In particular, observed decreases in diffusivity seen for tumors, such as lymphoma or small round blue cell tumors, may be related to their high cellularity (Stadnik et al., 2001). In the case of bacterial abscesses, observed decreases in diffusivity are likely related to an increase in proteinaceous content from suppurative exudate (Guzman et al., 2002). In PKU decreases in apparent diffusivity could be due to myelin damage from status spongiosis (Phillips et al., 2001) or the accumulation of intracellular debris produced as a byproduct of inadequate phenylalanine metabolism (Leuzzi et al., 2007). For some of the above diseases, changes in diffusivity can occur symmetrically in both AD and RD such that no observable changes are seen in FA. In regards to HIV, observed decreases in AD, RD, and MD seen in HIV+/cART subjects may reflect macrophages and microglia infiltration due to active viral replication within the CNS or cytotoxic edema. The presence of inflammatory cells and surrounding debris could decrease the free path of water diffusion (Wang et al., 2011).

Normalization of DTI diffusivity parameters was seen in HIV+ subjects receiving long-term cART as well as some HIV+ participants who had more recently initiated cART. Initiation of cART could lead to a reduction in viral replication and a corresponding decrease in inflammatory cells and edema within the CNS. Observed changes in DTI parameters may be more sensitive to inflammatory changes compared to neuropsychological testing as similar cognitive performance values were observed before and after starting cART. Additional studies are required correlating DTI parameters with cerebral spinal fluid measurements of HIV viral load and inflammation.

The current study has several limitations. First, our study focused on a limited number of regions. The CC and CSO were chosen as these WM regions can be easily delineated and have been previously investigated in DTI studies (Chang et al., 2008; Filippi et al., 2001; Pfefferbaum et al., 2007; Pomara et al., 2001; Ragin et al., 2005; Thurnher et al., 2005; Wu et al., 2006). Future studies that include additional white matter regions would allow us to determine if observed changes are particular to certain WM regions or if changes occurring throughout the brain. Second, we were unable to differentiate the efficacy of cART in the CNS based on CPE scores as most participants received only a limited number of regimens due to both patient and provider preferences. The relative degree of improvements in DTI parameters could be influenced by cART penetration into the CNS. Further studies investigating the effects of CPE on DTI measures are therefore needed. This study also cannot distinguish when an individual should initiate therapy as only chronically HIV

infected patients were studied. Additional studies of acute and early HIV+ patients initiating cART should be performed.

4.1 Conclusions

The data presented here further support the use of DTI to assist in understanding the effects of HIV on WM structural integrity. Our results support the use of a cART for treating HIV+ individuals, as some HIV+ subjects initiating therapy have improvements in DTI parameters that are comparable to those seen in HIV- individuals.

Acknowledgments

The authors would like to thank Drs. Tammie Benzinger and Florin Vaida for their suggestions and comments throughout the study. Funding support came from the National Institute of Mental Health (NIMH) (K23MH081786) (BMA), National Institute of Nursing Research (NINR) (R01NR012907 and R01NR012657) (BMA), and the Dana Foundation (DF10052) (BMA).

References

Ances BM, Ellis RJ. Dementia and neurocognitive disorders due to HIV-1 infection. Semin Neurol. 2007; 27(1):86–92. [PubMed: 17226745]

Antinori A, Arendt G, Becker JT, Brew BJ, Byrd DA, Cherner M, Wojna VE. Updated research nosology for HIV-associated neurocognitive disorders. Neurology. 2007; 69(18):1789–1799. [PubMed: 17914061]

Bozzali M, Falini A, Franceschi M, Cercignani M, Zuffi M, Scotti G, Filippi M. White matter damage in Alzheimer's disease assessed in vivo using diffusion tensor magnetic resonance imaging. J Neurol Neurosurg Psychiatry. 2002; 72(6):742–746. [PubMed: 12023417]

Cardenas VA, Meyerhoff DJ, Studholme C, Kornak J, Rothlind J, Lampiris H, Weiner MW. Evidence for ongoing brain injury in human immunodeficiency virus-positive patients treated with antiretroviral therapy. J Neurovirol. 2009; 15(4):324–333. [PubMed: 19499454]

Chang L, Wong V, Nakama H, Watters M, Ramones D, Miller EN, Ernst T. Greater than age-related changes in brain diffusion of HIV patients after 1 year. J Neuroimmune Pharmacol. 2008; 3(4):265–274. [PubMed: 18709469]

Chanraud S, Zahr N, Sullivan EV, Pfefferbaum A. MR diffusion tensor imaging: a window into white matter integrity of the working brain. Neuropsychol Rev. 2010; 20(2):209–225. [PubMed: 20422451]

Chen Y, An H, Zhu H, Stone T, Smith JK, Hall C, Lin W. White matter abnormalities revealed by diffusion tensor imaging in non-demented and demented HIV+ patients. Neuroimage. 2009; 47(4): 1154–1162. [PubMed: 19376246]

Filippi CG, Ulug AM, Ryan E, Ferrando SJ, van Gorp W. Diffusion tensor imaging of patients with HIV and normal-appearing white matter on MR images of the brain. AJNR. 2001; 22(2):277–283. [PubMed: 11156769]

Gongvatana A, Schweinsburg BC, Taylor MJ, Theilmann RJ, Letendre SL, Alhassoon OM, Grant I. White matter tract injury and cognitive impairment in human immunodeficiency virus-infected individuals. J Neurovirol. 2009; 15(2):187–195. [PubMed: 19306228]

Gongvatana A, Cohen RA, Correia S, Devlin KN, Miles J, Kang H, Tashima KT. Clinical contributors to cerebral white matter integrity in HIV-infected individuals. J Neurovirol. 2011; 17(5):477–486. [PubMed: 21965122]

Guzman R, Barth A, Lovblad KO, El-Koussy M, Weis J, Schroth G, Seiler RW. Use of diffusion-weighted magnetic resonance imaging in differentiating purulent brain processes from cystic brain tumors. Journal of Neurosurgery. 2002; 97(5):1101–1107. [PubMed: 12450032]

Heaton RK, Franklin DR, Ellis RJ, McCutchan JA, Letendre SL, Leblanc S, Wolfson T. HIV-associated neurocognitive disorders before and during the era of combination antiretroviral therapy: differences in rates, nature, and predictors. J Neurovirol. 2011; 17(1):3–16. [PubMed: 21174240]

Kuper M, Rabe K, Esser S, Gizewski ER, Husstedt IW, Maschke M, Obermann M. Structural gray and white matter changes in patients with HIV. J Neurol. 2011; 258(6):1066–1075. [PubMed: 21207051]

Letendre SL, Ellis RJ, Ances BM, McCutchan JA. Neurologic complications of HIV disease and their treatment. Top HIV Med. 2010; 18(2):45–55. [PubMed: 20516524]

Li C, Zhang X, Komery A, Li Y, Novembre FJ, Herndon JG. Longitudinal diffusion tensor imaging and perfusion MRI investigation in a macaque model of neuro-AIDS: a preliminary study. Neuroimage. 2011; 58(1):286–292. [PubMed: 21658455]

Muller-Oehring EM, Schulte T, Rosenbloom MJ, Pfefferbaum A, Sullivan EV. Callosal degradation in HIV-1 infection predicts hierarchical perception: a DTI study. Neuropsychologia. 2010; 48(4): 1133–1143. [PubMed: 20018201]

Narciso P, Galgani S, Del Grosso B, De Marco M, De Santis A, Balestra P, Tozzi V. Acute disseminated encephalomyelitis as manifestation of primary HIV infection. Neurology. 2001; 57(8):1493–1496. [PubMed: 11673598]

Pfefferbaum A, Rosenbloom MJ, Adalsteinsson E, Sullivan EV. Diffusion tensor imaging with quantitative fibre tracking in HIV infection and alcoholism comorbidity: synergistic white matter damage. Brain. 2007; 130(Pt 1):48–64. [PubMed: 16959813]

Pfefferbaum A, Rosenbloom MJ, Rohlfing T, Kemper CA, Deresinski S, Sullivan EV. Frontostriatal fiber bundle compromise in HIV infection without dementia. AIDS. 2009; 23(15):1977–1985. [PubMed: 19730350]

Phillips MD, McGraw P, Lowe MJ, Mathews VP, Hainline BE. Diffusion-weighted imaging of white matter abnormalities in patients with phenylketonuria. AJNR. 2001; 22(8):1583–1586. [PubMed: 11559511]

Pomara N, Crandall DT, Choi SJ, Johnson G, Lim KO. White matter abnormalities in HIV-1 infection: a diffusion tensor imaging study. Psychiatry Res. 2001; 106(1):15–24. [PubMed: 11231096]

Ragin AB, Storey P, Cohen BA, Edelman RR, Epstein LG. Disease burden in HIV-associated cognitive impairment: a study of whole-brain imaging measures. Neurology. 2004; 63(12):2293–2297. [PubMed: 15623689]

Ragin AB, Storey P, Cohen BA, Epstein LG, Edelman RR. Whole brain diffusion tensor imaging in HIV-associated cognitive impairment. AJNR. 2004; 25(2):195–200. [PubMed: 14970017]

Ragin AB, Wu Y, Storey P, Cohen BA, Edelman RR, Epstein LG. Diffusion tensor imaging of subcortical brain injury in patients infected with human immunodeficiency virus. J Neurovirol. 2005; 11(3):292–298. [PubMed: 16036809]

Rimkus Cde M, Junqueira Tde F, Lyra KP, Jackowski MP, Machado MA, Miotto EC, Leite Cda C. Corpus callosum microstructural changes correlate with cognitive dysfunction in early stages of relapsing-remitting multiple sclerosis: axial and radial diffusivities approach. Mult Scler Int. 2011; 12:275–283.

Shimony JS, Burton H, Epstein AA, McLaren DG, Sun SW, Snyder AZ. Diffusion tensor imaging reveals white matter reorganization in early blind humans. Cereb Cortex. 2006; 16(11):1653–1661. [PubMed: 16400157]

Shimony JS, Sheline YI, D'Angelo G, Epstein AA, Benzinger TL, Mintun M, Snyder AZ. Diffuse microstructural abnormalities of normal-appearing white matter in late life depression: a diffusion tensor imaging study. Biol Psychiatry. 2009; 66(3):245–252. [PubMed: 19375071]

Song SK, Sun SW, Ramsbottom MJ, Chang C, Russell J, Cross AH. Dysmyelination revealed through MRI as increased radial diffusion of water. NeuroImage. 2002; 17(3):1429–1436. [PubMed: 12414282]

Song SK, Sun SW, Ju WK, Lin SJ, Cross AH, Neufeld AH. Diffusion tensor imaging detects and differentiates axon and myelin degeneration in mouse optic nerve after retinal ischemia. NeuroImage. 2003; 20(3):1714–1722. [PubMed: 14642481]

Stadnik TW, Chaskis C, Michotte A, Shabana WM, van Rompaey K, Luypaert R, Osteaux M. Diffusion-weighted MR imaging of intracerebral masses: comparison with conventional MR imaging and histologic findings. AJNR. 2001; 22(5):969–976. [PubMed: 11337344]

Stebbins GT, Smith CA, Bartt RE, Kessler HA, Adeyemi OM, Martin E, Moseley ME. HIV-associated alterations in normal-appearing white matter: a voxel-wise diffusion tensor imaging study. J Acquir Immune Defic Syndr. 2007; 46(5):564–573. [PubMed: 18193498]

Sullivan EV, Rosenbloom MJ, Rohlfing T, Kemper CA, Deresinski S, Pfefferbaum A. Pontocerebellar contribution to postural instability and psychomotor slowing in HIV infection without dementia. Brain Imaging Behav. 2011; 5(1):12–24. [PubMed: 20872291]

Tate DF, Sampat M, Harezlak J, Fiecas M, Hogan J, Dewey J, Navia B. Regional areas and widths of the midsagittal corpus callosum among HIV-infected patients on stable antiretroviral therapies. J Neurovirol. 2011; 17(4):368–379. [PubMed: 21556960]

Thurnher MM, Castillo M, Stadler A, Rieger A, Schmid B, Sundgren PC. Diffusion-tensor MR imaging of the brain in human immunodeficiency virus-positive patients. AJNR. 2005; 26(9): 2275–2281. [PubMed: 16219833]

Towgood KJ, Pitkanen M, Kulasegaram R, Fradera A, Kumar A, Soni S, Kopelman MD. Mapping the brain in younger and older asymptomatic HIV-1 men: Frontal volume changes in the absence of other cortical or diffusion tensor abnormalities. Cortex. 2011 in press.

Tross S, Price RW, Navia B, Thaler HT, Gold J, Hirsch DA, Sidtis JJ. Neuropsychological characterization of the AIDS dementia complex: a preliminary report. AIDS. 1988; 2(2):81–88. [PubMed: 3132951]

Turner MR, Modo M. Advances in the application of MRI to amyotrophic lateral sclerosis. Expert Opin Med Diagn. 2010; 4(6):483–496. [PubMed: 21516259]

Van Gorp WG, Miller EN, Satz P, Visscher B. Neuropsychological performance in HIV-1 immunocompromised patients: a preliminary report. Journal of clinical and experimental neuropsychology. 1989; 11(5):763–773. [PubMed: 2808663]

Wang Y, Wang Q, Haldar JP, Yeh FC, Xie M, Sun P, Song SK. Quantification of increased cellularity during inflammatory demyelination. Brain. 2011; 134(Pt 12):3587–3598.

White DA, Connor LT, Nardos B, Shimony JS, Archer R, Snyder AZ, McKinstry RC. Age-related decline in the microstructural integrity of white matter in children with early- and continuously-treated PKU: a DTI study of the corpus callosum. Mol Genet Metab. 2010; 99(1):S41–46. [PubMed: 20123469]

Wu Y, Storey P, Cohen BA, Epstein LG, Edelman RR, Ragin AB. Diffusion alterations in corpus callosum of patients with HIV. AJNR. 2006; 27(3):656–660. [PubMed: 16552012]

Abbreviations

DTI	Diffusion Tensor Imaging
WM	White Matter
CC	Corpus Callosum
CSO	Centrum Semiovale
cART	Combination Antiretroviral Therapy

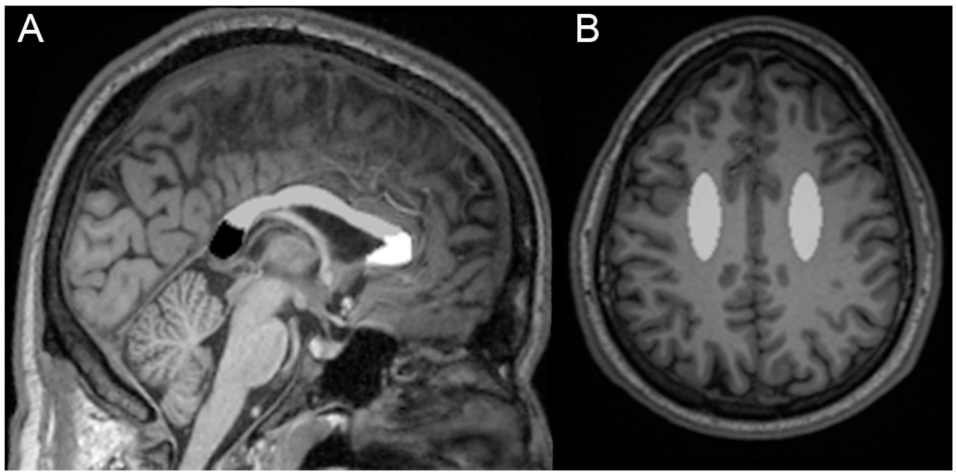

Figure 1.

Regions on T1-weighted three-dimensional magnetization-prepared rapid acquisition gradient echo (MPRAGE) images from a HIV infected (HIV+) participant naïve to combination anti-retroviral therapy (cART). a) Regions of the corpus callosum (CC) are delineated. The dotted line outlines the CC on a sagittal slice. *Black*: Splenium of the CC; *Gray*: Body of the CC; *White*: Genu of the CC. B) Manual region of interest for the centrum semiovale (CSO) in gray.

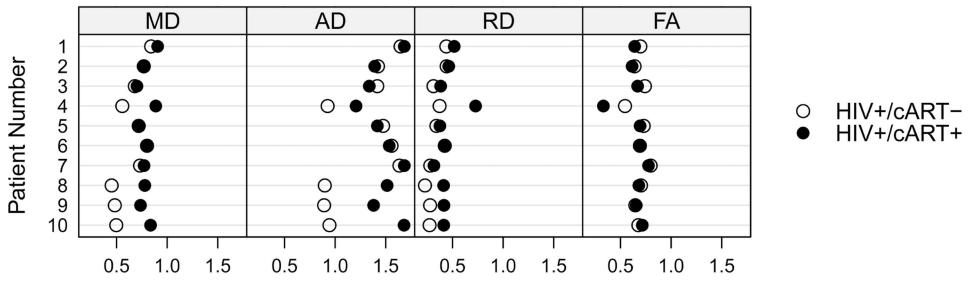

Figure 2.
Longitudinal analysis for ten HIV+ subjects both immediately before and approximately 6 months after receiving stable cART regimen.

AIDS. Author manuscript; available in PMC 2013 August 25.

Table 1

Demographic, medical, neuropsychological, and laboratory values for all subjects.

	HIV- (n=21)	HIV+/cART+ (n=21)	HIV+/cART- (n=21)
Age (years)	39 (12)	41 (14)	38 (13)
Education (years)	13 (2)	13 (3)	13 (2)
Sex (% male)	91	91	91
CD4 (cells/μL)	N/A	384 (264, 583)	371 (278, 474)
CD4 nadir (cells/μL)	N/A	127 (27, 293)	320 (228, 411)[a]
Log Plasma HIV viral Load	N/A	1.93 (0.50)	3.95 (0.84)[a]
% Virologically suppressed (% <50 copies/mL)	N/A	71	N/A
NPZ-4 score	−0.21 (0.96)	−0.50 (1.2)	−0.70 (0.77)
Self –reported duration of Infection (months)	N/A	54 (56)	18 (18)[a]
Duration on cART (months)	N/A	25 (23)	N/A

All errors are reported as standard deviation of the mean, and quartiles for laboratory values.
cART: combination antiretroviral therapy, NPZ-4: neuropsychological performance z score

[a]HIV+/cART- vs HIV+/ART-, $p \leq 0.02$.

AIDS. Author manuscript; available in PMC 2013 August 25.

Table 2

DTI parameters sampled from the corpus callosum (CC) (genu, body, splenium) and centrum semiovale (CSO).

	HIV-	HIV+/cART+	HIV+/cART-
Mean Diffusivity (MD)			
Genu of CC	0.7661 (0.087)[a]	0.8374 (0.097)[b]	0.6750 (0.160)
Body of CC	0.8055 (0.097)[a]	0.8534 (0.071)[b]	0.6932 (0.161)
Splenium of CC	0.7130 (0.096)[a]	0.7396 (0.063)[b]	0.6141 (0.155)
CSO	0.6415 (0.031)[a]	0.6863 (0.062)[b]	0.5577 (0.134)
Fractional Anisotropy (FA)			
Genu of CC	0.6373 (0.125)	0.6254 (0.095)	0.6757 (0.056)
Body of CC	0.6013 (0.103)	0.6141 (0.088)	0.6493 (0.060)
Splenium of CC	0.7128 (0.098)	0.7345 (0.061)	0.7454 (0.042)
CSO	0.4392 (0.045)	0.4288 (0.059)	0.4443 (0.052)
Axial Diffusivity (AD)			
Genu of CC	1.4248 (0.202)	1.5238 (0.185)[b]	1.2919 (0.313)
Body of CC	1.4310 (0.167)[a]	1.5200 (0.164)[b]	1.2789 (0.286)
Splenium of CC	1.4293 (0.169)[a]	1.5301 (0.140)[b]	1.2831 (0.340)
CSO	0.9729 (0.056)[a]	1.0288 (0.068)[b]	0.8299 (0.207)
Radial Diffusivity (RD)			
Genu of CC	0.4368 (0.116)[a]	0.4943 (0.105)[b]	0.3666 (0.102)
Body of CC	0.4927 (0.119)[a]	0.5151 (0.094)[b]	0.4003 (0.112)
Splenium of CC	0.3549 (0.119)[a]	0.3495 (0.055)[b]	0.2796 (0.076)
CSO	0.4758 (0.036)[a]	0.5151 (0.070)[b]	0.4216 (0.104)

Mean (SD); CC: Corpus Callosum; CSO: Centrum Semiovale

[a] HIV- vs. HIV+/cART-, $p \leq 0.03$

[b] HIV+/cART+ vs. HIV+/cART-, $p \leq 0.002$.